

## Aerodynamic Shape Optimization using Discrete Adjoint Formulation based on Overset Mesh System

Byung Joon Lee\*, Jin Woo Yim\*\*, Jun Sok Yi\*\*\* and Chongam Kim\*\*\*\*

School of Mechanical and Aerospace Engineering  
Seoul National University, Seoul, Korea 151-742

### Abstract

A new design approach of complex geometries such as wing/body configuration is arranged by using overset mesh techniques under large scale computing environment. For an in-depth study of the flow physics and highly accurate design, several special overlapped structured blocks such as collar grid, tip-cap grid, and etc. which are commonly used in refined drag prediction are adopted to consider the applicability of the present design tools to practical problems. Various pre- and post-processing techniques for overset flow analysis and sensitivity analysis are devised or implemented to resolve overset mesh techniques into the design optimization problem based on Gradient Based Optimization Method (GBOM). In the pre-processing, the convergence characteristics of the flow solver and sensitivity analysis are improved by overlap optimization method. Moreover, a new post-processing method, Spline-Boundary Intersecting Grid (S-BIG) scheme, is proposed by considering the ratio of cell area for more refined prediction of aerodynamic coefficients and efficient evaluation of their sensitivities under parallel computing environment. With respect to the sensitivity analysis, discrete adjoint formulations for overset boundary conditions are derived by a full hand-differentiation. A smooth geometric modification on the overlapped surface boundaries and evaluation of grid sensitivities can be performed by mapping from planform coordinate to the surface meshes with Hicks-Henne function. Careful design works for the drag minimization problems of a transonic wing and a wing/body configuration are performed by using the newly-developed and -applied overset mesh techniques. The results from design applications demonstrate the capability of the present design approach successfully.

**Key Word :** Discrete Adjoint Approach, Overset Mesh Technique, Optimal Shape Design, S-BIG(Spline-Boundary Intersection Grid), Complex Geometry

### Introduction

The aerodynamic shape optimizations(ASO) of multiple body aircraft geometries with adjoint approach have been a matter of concerning since late 1990s.[1, 2] Design methods by using multi-block system do not require any additional techniques as compared with single block problems. Therefore, a straightforward extension of single block design tools is carried out to resolve the design problems of wing/body configurations and full body supersonic aircraft by numerous researchers.[3-5] Multi-block mesh system can secure a good grid quality. However, in

---

\* Postdoctoral Research Associate

\*\* Ph. D. Candidate

\*\*\* M. S. Candidate Associate Professor

\*\*\*\* Associate Professor, General Manager (Institute of Advanced Aerospace Technology, SNU)  
E-mail : chongam@snu.ac.kr Tel : 02-880-1915 Fax : 02-887-2662

the cases of moving grid problems and deforming grid applications, a large amount of shape changes are inevitable and sometimes the grid topology should be changed. In these cases, the design optimization works cannot be performed fully automatically on the multi-block system. On the other hand, in case of unstructured mesh system, the automatic mesh deformation can be an easy work. For this reason, unstructured discrete adjoint solvers are developed by, Nielsen(1998)[6], Kim(2000)[7] Mavriplis(2007)[8] et al. Nevertheless, compared with the structured grid, far more grid points are needed to analyze the flow in keeping the same resolution of solution. Additionally, it requires much more computing memory and computational time cost than the structured grid demands even with the same number of grid points.

In view of these issues, the overset grid technique has several benefits to be applied to the large scale flow analysis and design optimization problems. First, the grid topology is relatively simple enough to represent the flexible deformation of mesh system without changing the block topology. Second, the movement of the grids, the change of the part position, and the exchange of parts are easily implemented. Third, highly-resolved flow solutions can be obtained via a relatively small number of grid points. Finally, a fully automatic grid-generation is possible because of the simple grid topology. These characteristics of overset mesh technique can derive the design optimization to the final goal, *'fully automatic aerodynamic design from CAD models'*. However, the development of adjoint solvers based on overset mesh system is carried out by only a few researchers. Multi-element airfoil design with hand-differentiated discrete adjoint solver is performed by Kim et al.[9] with respect to the turbulent flows. In case of three-dimensional case, an aerodynamic shape optimization for a simple turbine vane is carried out by Liao et al. They applied continuous adjoint formulation for Euler-equations by using implicit hole-cutting method to the design work.[10]

In the present paper, we applied several major pre- and post-processing methods for overset mesh system to an aerodynamic shape design tool based on discrete adjoint approach. These techniques are newly devised or arranged for the sensitivity analysis and design problems. Thus, Spline-Boundary Interpolation Grid(S-BIG) scheme for efficient calculation of aerodynamic coefficients and their derivatives. The overlap optimization[12] for high quality flow analysis results and good convergence characteristics of adjoint solver are resolved in the design optimization tools for complex geometries. The sensitivity analysis results are validated by comparison with the complex step derivatives for a transonic wing. Exploiting these techniques a drag minimization problem for a wing/body configurations with the overset grid system are carried out. [13]

## Numerical Techniques

### Overlap Optimization for Overset adjoint solver

As mentioned above, the main focus of the present work is the application of adjoint approach in discrete manner to the complex overset mesh system. Recently, there are many progresses in flow analysis techniques for overset mesh system. The main issues of the overset flow analysis codes are focused upon the preprocessors such as PEGSUS[12], DCF3D[14], BEGGAR[11, 15], Overture[16] and etc. These are high quality overset preprocessors to construct the connectivity of the overlapped blocks automatically. Especially, PEGASUS is one of the most efficient and robust code and a tremendous number of applications, i.e., flow analyses of very complex geometries as like full body aircraft, space craft, turbine blade, and so on, are carried out by using this preprocessing code in NASA. In these applications, the overlapped blocks are too many and the block connectivity of grid systems is inevitably so complicated to resolve the complicated flow phenomena with refined definition of analysis. As a result, an automatic process for hole-searching and construction of block connectivity are applied to the latest version. This technique is baptized by the name of overlap optimization. This method can improve the

convergence characteristics of overset analysis code by considering the ratio of cell volume or cell aspect ratio of donor and fringe cells. In addition, it can diminish the discrepancy of the overset solutions by minimizing overlapped different computation region in the same physical space. The present sensitivity analysis code in adjoint approach is definitely affected by the oscillation of the overset solution, too.

The basic concept of overlap optimization is presented in Fig. 1. In order to construct the block connectivity between three simple 1-D overset blocks having different grid distribution as shown in Fig. 1-(a), the flow variables in the overlapped region are calculated with the flux function and those of all the coarser cells are updated by the interpolation. For accurate and robust interpolation, the donor cells for each fringe cell are selected by considering the cell-difference parameter (CDP). The CDP is defined as:

$$CDP = \sum_{j=1}^3 \frac{(X_j)_{DB} V_B - (X_j)_{DI} V_I}{(X_j)_{DB} V_B} \quad (1)$$

where  $(X_j)_{DB}$  is the maximum of the  $j^{th}$  component of the four diagonals of the boundary cell (one of the candidates of the donor cell),  $(X_j)_{DI}$  is the maximum of the  $j^{th}$  component of the four diagonals of the interpolation cell (fringe cell),  $V_B$  is the volume of the minimum Cartesian cell encompassing the boundary cell, and  $V_I$  is the volume of the minimum Cartesian cell encompassing the interpolated cell. CDP will vary from 0 (the best) to very large values. [12]

Equation (1) comprises that this parameter can represent the difference of cell aspect ratio and cell volume simultaneously between the fringe and donor cells. In case that there is a region where the fringe cells of the block A and B are overlapped as shown in Fig. 1 - (b) and (c), the region is determined as computational domain by removing the relation of interpolation. Finally, the left region of block A and right region of block B will be the computational domain and other regions are updated by interpolation with the block connectivity in Fig. 1-(d). For more details about overlap optimization process, refer to Ref.[12]. Figure 2 shows the comparison of computational domain of the manually assigned case and overlap optimized case for fuselage block of DLR-F4 wing/body configuration. The overlapped computational regions where two or more solutions coexist in the same physical space are minimized.

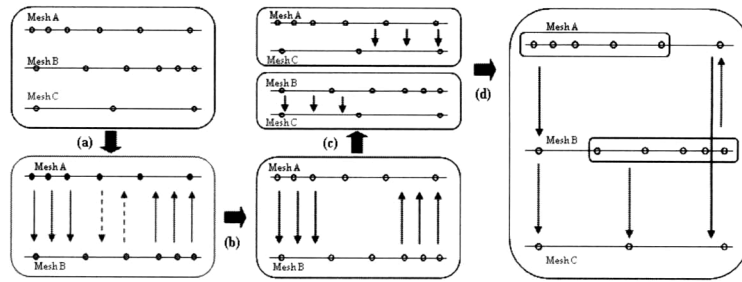


Fig. 1. Procedure of Overlap Optimization [12]

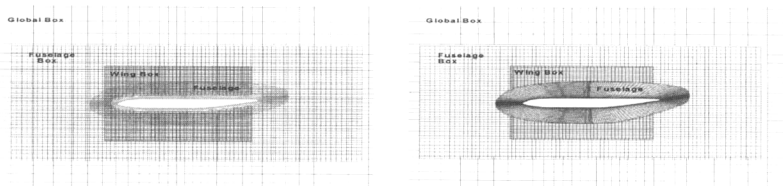


Fig. 2. Comparison of Computational Domain  
[Manually Assigned case(Left) and Overlap Optimized Case(Right)]

### Spline-Boundary Intersection Grid(S-BIG) Scheme

With regard to the post processor for overset flow analysis, Zipper grid scheme[17] is widely used in calculation of aerodynamic coefficients. Zipper grid scheme is a kind of grid reconstruction method. This method consists of blanking process of overlapped region and reconstruction process with an unstructured surface grid set. The flow variables on the zipper grid are interpolated from donor cells of computational overlapped blocks around the same physical point. However, the flux differential terms from arbitrary number of donor cells make it difficult to apply this method to the adjoint solver. In the present work, a newly devised Spline-Boundary Intersecting Grid (S-BIG) scheme is applied to the post processing routine and sensitivity analysis code for more efficient differentiation process. The objective of S-BIG is preparation of evaluating routines for aerodynamic coefficients that require no interpolation process from donor cells. If Zipper grid scheme is to reconstruct grids on the block level, S-BIG is to reconstruct grids on the cell level. As a result, to carry out the differentiation of the flux terms or the evaluation of aerodynamic coefficients, it does not require anything except the boundary information of the overlapped blocks. The procedure of S-BIG scheme can be summarized with the elimination of the overlapped surface cells and re-formation the cell vertices on the basis of prescribed spline boundary as shown in Fig.3. Each re-formed cell can be represented by a set of triangles as shown in the figure. The aerodynamic coefficients can be evaluated by using the area of surface meshes constructed by the re-formed surface cells.

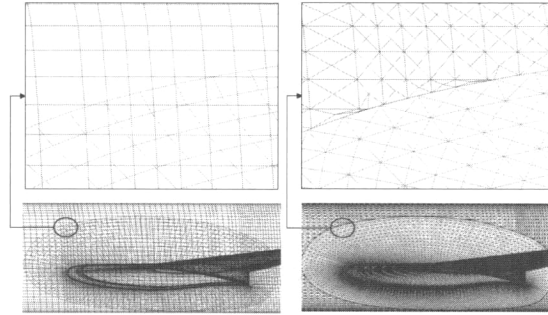


Fig. 3. Reformed Cell at the Fuselage and Collar Block Interface  
[Original Overset Surface Meshes(Left) and Reformed Surface Meshes(Right)]

### Sensitivity Analysis for Overset Boundary

The sensitivity of an objective function with respect to a design variable from discrete adjoint formulation can be evaluated by Eq. (2), (3) and (4). The sensitivities can be acquired with the grid sensitivities of objective functions and residual equations, and the adjoint vector  $\Lambda$  as shown in Eq. (2).

$$\left\{ \frac{dF}{dD} \right\} = \left\{ \frac{\partial F}{\partial X} \right\}^T \left\{ \frac{dX}{dD} \right\} + \left\{ \frac{\partial F}{\partial D} \right\} + \Lambda^T \left( \left[ \frac{\partial R}{\partial X} \right]^T \left\{ \frac{dX}{dD} \right\} + \left\{ \frac{\partial R}{\partial D} \right\} \right) \quad (2)$$

if and only if the adjoint vector  $\Lambda$  satisfies the following adjoint equation.

$$\left[ \frac{\partial R}{\partial Q} \right]^T \Lambda + \left\{ \frac{\partial F}{\partial Q} \right\} = \{0\} \quad (3)$$

The solution vector  $\Lambda$  is obtained by solving the Euler implicit method of Eqn. (3) time-iteratively as

$$\left( \frac{I}{J\Delta t} + \left[ \frac{\partial R}{\partial Q} \right]_{VL}^T \right) \Delta \Lambda = - \left[ \frac{\partial R}{\partial Q} \right]^T \Lambda^m - \left\{ \frac{\partial F}{\partial Q} \right\}^T \quad (4)$$

$$\Lambda^{m+1} = \Lambda^m + \Delta \Lambda \quad (\text{update vector } \Lambda \text{ of } (m+1)^{th} \text{ step})$$

where  $I$  is identity matrix, and  $J$  represents Jacobian matrix, and the subscript  $VL$  means the Van-Leer flux Jacobian.

The adjoint equation (4) is solved by a time integration scheme with the boundary conditions of Eqn. (5), (6).

$$\left[ \frac{\partial R}{\partial Q} \right]^T \Lambda + \left[ \frac{\partial R_B}{\partial Q} \right]^T \Lambda_B + \left\{ \frac{\partial F}{\partial Q} \right\}^T = \{0\}^T \quad (5)$$

$$\left[ \frac{\partial R}{\partial Q_B} \right]^T \Lambda + \left[ \frac{\partial R_B}{\partial Q_B} \right]^T \Lambda_B + \left\{ \frac{\partial F}{\partial Q} \right\}^T = \{0\}^T \quad (6)$$

where subscript  $B$  represents boundary cell. In Eqn.(5), adjoint variable  $\Lambda_B$  of boundary cell is updated by inner cell-values of  $n$ -th time step. And the variables of the next time step ( $n+1$ ) are evaluated by Eqn.(5) using the boundary values from (6). Overset boundary conditions can be derived by a similar way to the conventional adjoint boundary conditions except the number of equations as like Eqn. (7)–(10).

$$\left[ \frac{\partial R^M}{\partial Q^M} \right]^T \Lambda^M + \left[ \frac{\partial R_F^S}{\partial Q^M} \right]^T \Lambda_F^S + \left\{ \frac{\partial F^M}{\partial Q^M} \right\}^T = \{0\}^T \quad (7)$$

$$\left[ \frac{\partial R^S}{\partial Q^S} \right]^T \Lambda^M + \left[ \frac{\partial R_F^M}{\partial Q^S} \right]^T \Lambda_F^M + \left\{ \frac{\partial F^S}{\partial Q^S} \right\}^T = \{0\}^T \quad (8)$$

$$\left[ \frac{\partial R^M}{\partial Q_F^M} \right]^T \Lambda^M + \left[ \frac{\partial R_F^M}{\partial Q_F^M} \right]^T \Lambda_F^M + \left\{ \frac{\partial F^M}{\partial Q_F^M} \right\}^T = \{0\}^T \quad (9)$$

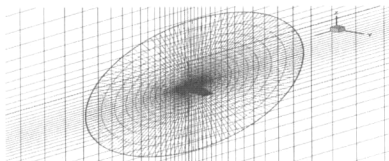
$$\left[ \frac{\partial R^S}{\partial Q_F^S} \right]^T \Lambda^S + \left[ \frac{\partial R_F^S}{\partial Q_F^S} \right]^T \Lambda_F^S + \left\{ \frac{\partial F^S}{\partial Q_F^S} \right\}^T = \{0\}^T \quad (10)$$

where the subscript  $F$  represent fringe cells and the superscript  $M$  and  $S$  represent the main grid and sub-grid domain respectively. Through the system equations, each overset boundary values can be updated to inner adjoint variables of the next time step. Inner values of sub-grid domain are evaluated by Eqn. (9), (8) orderly. And for the main-grid domain calculations are carried out from (10) to (7).

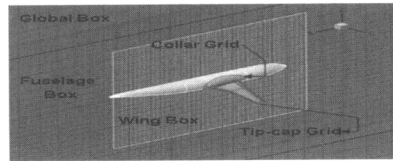
## Flow Analysis

### Overset Mesh system for Design problem

For the design optimization, two test geometries are adopted. 2 block-system of ONERA-M6 wing is used in the validation of the overset solver and the adjoint solver. The mesh system consists of wing block ( $143 \times 39 \times 33$ ) and global box block ( $63 \times 27 \times 63$ ). The wing block is O-O type grid and the box grid is a Cartesian grid as shown in Fig. 4-(a). The total number of mesh points is about 300 thousands pts.



(a) ONERA-M6 (2 Blocks)



(b) DLR-F4 (7 Blocks)

Fig. 4. Overset Mesh System for the Tset Case

A wing/body configuration is applied for more practical complicated problem. In the 1<sup>st</sup> Drag Prediction Workshop (DPWI), the provided test geometry of drag prediction is DLR-F4, which consists of wing and fuselage. [2, 13] Figure 4-(b) shows the overall mesh system of 7 blocks over DLR-F4. Those 7 blocks are global box ( $77 \times 38 \times 72$ ), fuselage box ( $84 \times 26 \times 45$ ), wing box ( $44 \times 37 \times 54$ ), fuselage block ( $190 \times 41 \times 30$  : O-O type), collar block ( $146 \times 26 \times 26$  : O-H type), wing block ( $143 \times 43 \times 34$  : O-H type), and tipcap block ( $103 \times 43 \times 42$  : C-type). All the box blocks are Cartesian grids. The total number of mesh points (7 blocks) is about 1.22 million. To guarantee a good mesh quality, collar block is positioned at the interface of wing and fuselage and tipcap block on the wing tip. The fuselage block is made up of 1 block by using untrimmed approach. The overset mesh systems used in the present work are shown in Fig. 4-(a) and (b).

### Numerical Techniques and Flow Analysis Results

The flow conditions for ONERA-M6 wing are that the free stream Mach number is 0.84 and the angle of attack is 3.06 degree, which is a well-known case where the lambda shock is observed on the wing surface. Those of DLR-F4 are that free stream Mach number is 0.75 and angle of attack is 0.0 degree. Those flow conditions are a validation case of DPW-I.

The governing equations are the three-dimensional compressible Euler equations. The governing equations are transformed in generalized coordinates and are solved with a finite-volume method. For the calculation of residual, convective terms are upwind-differenced based on RoeM scheme by Kim et al.[19] A MUSCL (Monotone Upstream Centered Scheme for Conservation Laws) approach using a third order interpolation is used to obtain a higher order of spatial accuracy in all calculations. For temporal integration, Yoon's LU-SGS scheme is applied.

The flow analysis results in Fig. 5 show the overlap optimization can secure the convergence characteristics of the flow solver and guarantee more refined solutions. The solution of overlap optimized case converges well until the residual is diminished to  $10^{-6}$  based on the initial errors. The flow analysis results of the two tests cases using the present numerical

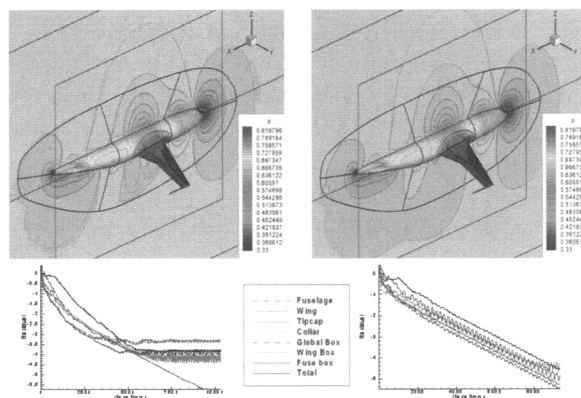
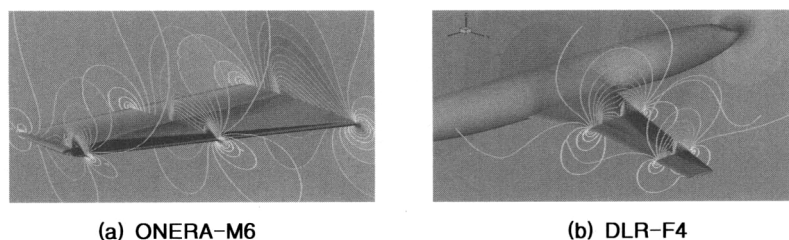


Fig. 5. Comparison of Flow Analysis Results without(Left) and with(Right) Overlap Optimization



(a) ONERA-M6

(b) DLR-F4

Fig. 6. Flow Analysis Results (Pressure Contours)

techniques are shown in Fig. 11. Those show that the interpolation between the overlapped blocks is carried out very well. In both of the cases, a complex shock configuration is observed on the upper wing surface and drag minimization will be presented through weakening the shock-strength in the next chapter.

## Design Optimization

### Validation of Sensitivity Analysis

The convergence characteristics of adjoint solver cannot be secured without the overlap optimization, either. Because the major premise of the adjoint approach is that the flow solutions should be well converged and the residual on each cell be almost zero. The convergence characteristics for adjoint solver with and without overlap optimization for ONERA-M6 wing with 2-blocks overset system are compared in Fig. 7(Left). This figure shows that manual hole-cutting and donor finding routines cannot secure stable convergence of the adjoint solver. And the overset adjoint solver is tested in 7 block system of DLR-F4 wing/body configuration to validate the sensitivity code in a complicated overset mesh system. The residual history shows that the adjoint solver converges very well on all the blocks in Fig. 7(Right).

The design variables used in the validation of overset adjoint solver are 20 Hicks-Henne functions on each design section of ONERA-M6 wing. 10 Hicks-Henne functions are imposed on upper and lower surface, respectively for each design section. The geometric modification is performed on 3 design sections at wing root, mid point, and wing tip. The deformation of other wing sections is evaluated by the linear-interpolation from the design sections. Totally, the number of the design variables used is 60. The gradient values of lift and drag coefficients for each design variable from adjoint approach are compared with the complex step derivatives (step size  $10^{-8}$ ) in Fig.8.[20] All the gradients agree very well with the complex step derivatives.

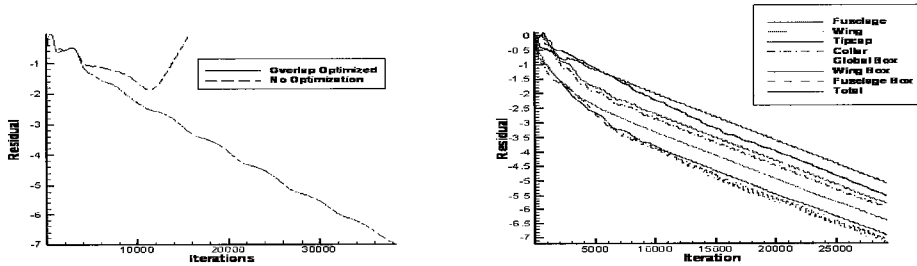


Fig. 7. Residual History of Overlap Optimized Overset adjoint solver [Left: 2 Block Overset Mesh(ONERA-M6), Right: 7 Block Overset Mesh(DLR-F4)]

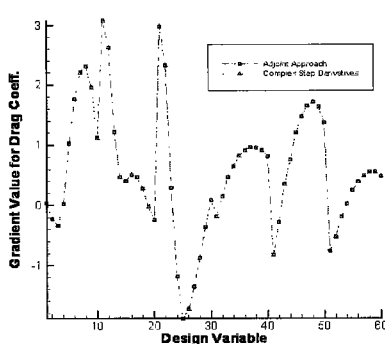


Fig. 8. Validation of Sensitivity Analysis

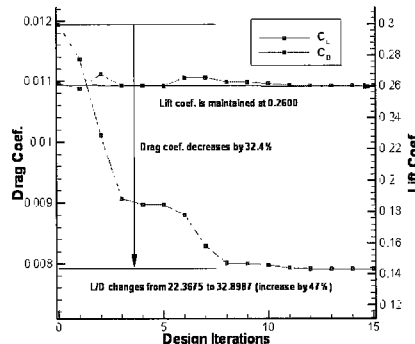


Fig. 9. Design History (ONERA-M6)

## Drag Minimization of Transonic Aircraft Geometries

The presented overset design approach is applied to design optimization of a transonic wing and W/B configuration. Optimization is performed by using the Broydon-Fletcher-Goldfarb-Shanno (BFGS) variable metric method which is a kind of non-constrained optimization technique. For the first application of overset GBOM tool, a shock-free problem on a transonic wing, ONERA-M6, is performed by minimization of drag with maintaining a constant lift coefficient. This problem is very common problem for the performance test of GBOM tool. The number of design variables used in this problem is 60 which is the same number to that of the validation case. The design problem is defined by Eq. (11). And as well known, the lift constraint is given by a form of penalty function as like Eq. (12) to prevent computational ineffectiveness of sensitivity analysis using adjoint approach. To guarantee the balanced variation of objective function and the penalty function, the weighting factor for the lift constraint is given by the ratio of the sensitivities of lift coefficient and drag coefficient for angle of attack.

Minimize :  $C_D$

$$\text{Subjected to : } C_L \geq C_{L_0}, \quad C_{L_0} = (\text{Lift Coefficient of Baseline Model}) \quad (11)$$

$$(\text{Object Function}) = C_D + Wt \times [0, C_{L_0} - C_L], \quad Wt = \frac{\partial C_D}{\partial \alpha} / \frac{\partial C_L}{\partial \alpha} \quad (12)$$

After completing the design process, the drag coefficient dramatically decreases as shown in Fig. 9. The design history shows the design process is converged well and the drag coefficient is changed from 0.0118 to 0.0079 (32% reduction) through 15 design iterations in maintaining lift coefficient at 0.2600. L/D is changed from 22.37 to 32.90 (47% increase). The pressure contours on the baseline ONERA-M6 wing and the designed wing are compared in Fig. 10. It can be observed that the shock on the wing upper surface decreases considerably. The  $C_p$  curves and shapes of wing sections on the designed wing notify that the flow acceleration right after leading edge decreases owing to the deformation of wing nose. And it can be induced through the  $C_p$  curves that the effect of wave drag on the surface is considerably diminished. Through the shock free problem of ONEAR-M6 wing, the present design tool show its capability and applicability to the transonic aerodynamic design problems.

For the next case, more complicated design problem of wing/body configuration with complex overset mesh system will be presented to validate the capability of the overset design tools in more practical usage. More complicated design work using 7 blocks of overset mesh system over a wing/body configuration is performed. Total 200 design variables on 10 design sections on wing surface are used. On each design section, 20 Hicks-Henne functions are used similarly to the transonic wing design problem. As mentioned before, there are three component blocks - collar block, wing block, and tipcap block - are overlapped on the wing surface. To

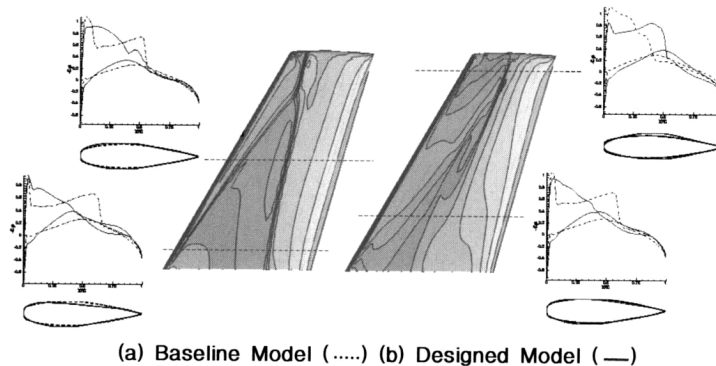


Fig. 10. Comparison of Surface Pressure Distribution

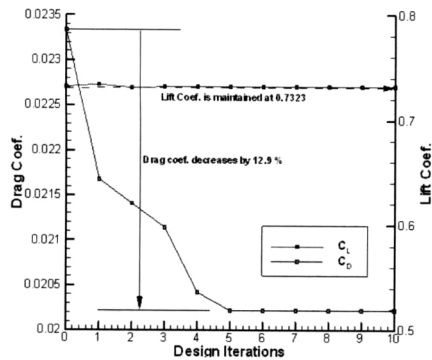
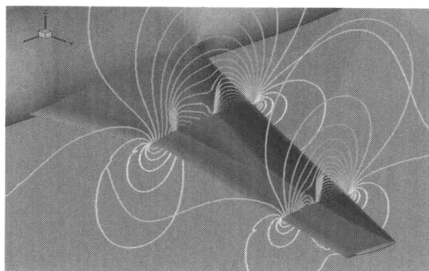


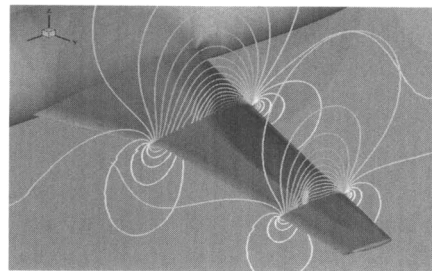
Fig. 11. Design History (DLR-F4)

Table 1. Drag Distribution on the Component

	Baseline	Designed Model	$\Delta(\%)$
Fuselage	6.3270E-03	6.3263E-03	-1%
Wing	1.6384E-02	1.383E-02	-17%



(a) Baseline Model (DLR-F4)



(b) Designed Model

Fig. 12. Comparison of Flow Pattern between Baseline Model and Design Model

deform the surface meshes during the design procedure, the overlapped meshes are mapped onto the planform. The deformation for the overlapped surface meshes which coexist on the same coordinate in the planform is equally. The design history in Fig. 11 shows that the drag is changed from 0.0227 to 0.0202 (12% reduction) through 10 design iterations. Considering the drag portion of fuselage, the quantity of its decrease is quite reasonable, because the quantity of drag decrease for wing only reaches about 17% as shown in table 1. The L/D is changed from 32.26 to 36.25 (12.3% increase). It is observed in Fig. 12 that the shock strength on the designed wing surface is diminished considerably. From the observation of design problems for transonic aircraft geometries, the present design tools for overset mesh system can be generally applied to the design problems of complex aircraft geometries.

## Conclusion

A new optimal design approach based on overset mesh technique and adjoint formulas. Especially, the overset boundary conditions for discrete adjoint approach are carefully derived. Overset flow analysis techniques are adequately adapted to the sensitivity analysis code and design modules by improvement or development. For the pre-processing of the overset flow analysis and sensitivity analysis, finding block connectivity is automatically carried out by overlap optimization. The improvement of convergence characteristics can be achieved in adjoint variable code through the overlap optimization. For the post-processing code, the aerodynamic coefficients are evaluated by Spline-Boundary Intersecting Grid Scheme (S-BIG) for convenient calculation of  $\{dF/dQ\}$  term in the sensitivity analysis. W.R.T. the grid modification in the design process, the overlapped surfaces of collar, wing, tipcap blocks can be displaced simultaneously by mapping from planform to wing surface. The present design approach with the special techniques for overset mesh system, successfully demonstrated its capability for the aerodynamic shape optimization of complex geometry design problems.

## Acknowledgement

The authors appreciate financial support by the Brain Korea-21 Project for the Mechanical and Aerospace Engineering Research at Seoul National University and by “the Smart UAV Development Program” of ‘the 21th Frontier R&D Program’ sponsored by the Ministry of Commerce, Industry and Energy.

## References

1. William M. Chan, Reynaldo J. Gomez III, Stuart E. Rogers, Pieter G. Buning. Best Practices in Overset Grid Generation. AIAA Paper 2002-3191
2. C. L. Rumsey, Robert T. Biedron. Computation of Flow Over a Drag Prediction Workshop Wing/Body Transport Configuration using CFL3D. NASA TM-2001-211262
3. K. Leoviriyakit, S. Kim, and A. Jameson. Viscous Aerodynamic Shape Design Optimization of Wings including Planform Variables. AIAA Paper 2003-3498.
4. S. Choi, J. J. Alonso, S. Kim, I. Kroo, and M. Wintzer. Two-Level Multi-Fidelity Design Optimization Studies for Supersonic Jets. AIAA Paper 2005-0531.
5. B. J. Lee, C. Kim, and O. Rho. Optimal Shape Design of the S-Shaped Subsonic Intake Using NURBS. AIAA Paper 2005-0455.
6. E. J. Nielsen, and W. K. Anderson. Aerodynamic Design Optimization on Unstructured Meshes Using the Navier-Stokes Equations. AIAA Paper 98-4809.
7. H. J. Kim, D. Sasaki, S. Obayashi, and K. Nakahashi. Aerodynamic Optimization of Supersonic Transport Wing Using Unstructured Adjoint Method. AIAA Journal, 2001, 39(6): 1011-1020.
8. S. Nadarajah, A. Jameson. Studies of the Continuous and Discrete Adjoint Approaches to Viscous Automatic Aerodynamic Shape Optimization. AIAA Paper 2001-2530.
9. C. S. Kim, Chongam Kim, O. H. Rho. Feasibility Study of Constant Eddy-Viscosity Assumption in Gradient-Based Design Optimization. Journal of Aircraft, 2003, 40(6):1168-1176.
10. W. Liao, and H. M. Tsai. Aerodynamic Design Optimization by the Adjoint Equation Method on Overset Grids. AIAA Paper 2006-54.
11. Ralph W. Noack, and Davy M. Belk. Improved Interpolation for Viscous Overset Grids. AIAA Paper 97-0199.
12. Norman E. Suhs, Stuart E. Rogers, and William E. Dietz. PEGASUS 5: An Automated Pre-processor for Overset-Grid CFD. AIAA Paper 2002-3186.
13. J. C. Vassberg, P. G. Buning, and C. L. Rumsey. Drag Prediction for the DLR-F4 Wing /Body using OVERFLOW and CFL3D on an Overset Mesh. AIAA Paper 2002-0840.
14. R. L. Meakin. Object X-rays for Cutting Holes in Composite Overset Structured Grids. AIAA Paper 2001-2537.
15. D. M. Belk, and R. C. Maple, “Automated Assembly of Structured Grids for Moving Body Problems”, AIAA Paper 95-1680.
16. D. L. Brown, W. D. Henshaw, and D. J. Quinlan. Overture: Object-Oriented Tools for Overset Grid Applications. AIAA Paper 99-3130.
17. W. M. Chan and P. G. Buning. Zipper Grids for Force and Moment Computation on Overset Grids. AIAA Paper 95-1681.
18. Nathan Hariharan, Z. J. Wang, and P. G. Buning. Application of Conservative Chimera Methodology in Finite Difference Settings. AIAA Paper 97-0627.
19. Sung-soo Kim, Chongam Kim, Oh-hyun Rho, and Seung Kyu Hong. Cures for the Shock Instability: Development of Shock-Stable Roe Scheme. Journal of Computational Physics, 2003, 185(2): 342-374.
20. J. R. R. A. Martins, I. M. Kroo, and J. J. Alonso. An Automated Method for Sensitivity Analysis using Complex Variables, AIAA Paper 2000-0869.